Samer Sahellie
Hartmut Pasternak

DOI: 10.1002/stab.201510294

Epoxy- and acrylic-bonded joints for strengthening lightweight steel girders

Several attempts have been made to introduce the adhesive bonding technique into steel construction, showing that this technique is promising and could replace traditional joining methods such as bolts, rivets and welding. Epoxy adhesive is used for structural joints more than acrylic due to its advanced properties such as its high capacity and its relatively good resistance to aging and environmental effects when compared with acrylic.
The following paper briefly shows the difference between the use of epoxy and acrylic adhesives when bonding steel plates to strengthen lightweight cold-formed galvanized steel girders. The thickness of the adhesive layers is 0.65 mm. Strengthened girders were tested experimentally at room temperature (20 °C) in 3-point bending tests and numerically investigated at –20 °C and +40 °C. The results show the efficiency of the bonded strengthening joints and that acrylic has an advantage in that it can absorb the deformations of the ductile steel without breaking.

Verstärkung von Stahlleichtbauprofilen durch Epoxid- und Acrylat-Klebverbindungen. *Bei der Untersuchung von Klebverbindungen im Stahlleichtbau hat sich gezeigt, dass diese Technik erfolgversprechend ist und die traditionellen Fügetechniken, wie Schrauben, Nieten und Schweißen, ersetzen kann. Epoxidklebstoff wird bei Stahlverbindungen häufiger verwendet als Acrylatklebstoff, da dieser bessere Eigenschaften wie hohe Festigkeit, relativ gute Alterungsbeständigkeit und Umweltauswirkungen hat.*
Der Beitrag zeigt am Beispiel der Verstärkung eines verzinkten Stahlleichtbauprofils den Unterschied zwischen Epoxid- und Acrylatklebstoffen. Die Dicke der Klebstoffschicht beträgt 0,65 mm. Der verstärkte Träger wird bei Raumtemperatur (20 °C) im 3-Punkt-Biegeversuch getestet und numerisch bei Temperaturen von –20 °C und +40 °C simuliert. Die Ergebnisse zeigen, dass die durch Kleben verstärkte Verbindung effektiv ist. Acrylat-Klebverbindungen haben den Vorteil, dass sie die Verformungen des duktilen Stahls ohne Bruch aufnehmen können.

1 Introduction

Epoxy and acrylic adhesives are commonly used in many structural applications. Epoxy generally has the highest strength properties. Intensive surface preparation and/or treatment are necessary to guarantee its durability. Epoxy can cure at room temperature but needs longer time unless it has been heated. After curing, it becomes rigid and its failure is rather brittle. Good strength properties with flexible form and ductile behaviour after relatively fast curing characterize acrylic adhesive. Its durability is guaranteed with moderate surface preparation and/or treatment. The selection of an appropriate adhesive for a specific application is essential and should be based on a good understanding of the differences between the adhesives available in terms of their behaviour, capacity, resistance to individual/combined loading and environmental influences, and their compatibility with the materials to be bonded.

Owing to the well-known problems associated with using traditional joining methods for lightweight steel structures, the adhesive bonding technique might be a good solution for joining such materials, especially considering that very good structural adhesives with improved properties are available nowadays.

Several studies have been conducted to introduce additional bonded plate reinforcement as a way of strengthening thin-gauge steel members ([1], [2], [3]). The results clearly confirm that this strengthening method is effective and that the load-carrying capacity of the structures can be increased.

A recent study [4] investigated the temperature effect on lap shear adhesive joints in lightweight steel structures. Two different adhesive systems (epoxy and acrylic) were tested within a temperature range of –20 °C to +40 °C. Short-term loading was applied to small-scale bonded specimens (with bondline thicknesses of 0.35 and 0.65 mm) and to large-scale bonded specimens (three patterns of strengthened C-section girders) with a bondline thickness of 0.65 mm. The small-scale bonded specimens were also investigated under long-term loading in order to understand the shear creep behaviour of such joints. The main results of this study show that acrylic has less resistance to the creep phenomenon than epoxy and that both of them are efficient when the bonded joints are subjected to short-term mechanical and thermal loading within the temperature range studied. This paper will show that for bonded strengthening joints in lightweight steel structures, if large bonded areas are used, then the stresses developing over most of the adhesive layer will be very small, so the risk resulting from the creep phenomenon will be negligible. Moreover, it will be shown that the steel structure fails prior to the adhesive failing. For the purpose of brevity, only some of the results from the 0.65 mm thick adhesives used in [4] as well as experimental and numerical

investigations at three temperatures on one pattern of the strengthened steel girders will be presented here.

2 Shear properties of adhesives studied

It is known that adhesive properties change depending on several effects such as temperature, humidity, aging and loading case. Therefore, these changes have to be determined and statistically treated in order to prove that the degradation of these properties is still within the permissible limits.

Figure 1 shows the temperature effect on shear properties of epoxy EP490 and acrylic DP810 (3M Scotch-Weld) used to bond double lap shear steel joints subjected to short-term loading, which represents the mean values obtained from seven specimens tested [4]. It is obvious from Figure 1a that the shear rigidity of both adhesives tends to decrease as the temperature rises and that epoxy is more rigid than acrylic at most of the temperatures studied. The same conclusion can be reached for the adhesives' shear capacity (maximum shear strength) (see Fig. 1b). The ductility, however, tends to increase when the temperature rises, as shown in Figure 1c. Moreover, it can be seen that the rigidity and ductility of acrylic are more strongly affected by the temperature. The degradation of the shear capacity of these adhesives over the temperature range from –20 to +40 °C has been statistically treated in [5]. As a consequence, the conversion factor η and the partial safety factor γ for the limit state have been determined according to [6] till [9]. The recommended factors are η = 0.69 and γ = 1.32.

Table 1. Normalized shear stress for 1, 5, 10 and 25 years
Tabelle 1. Bezogene Schubspannung für 1, 5, 10 und 25 Jahre

	(τ_{app}/τ_{max}) [%] *			
	1 year	5 years	10 years	25 years
AC-0.65	20.5	10.9	6.7	1.2
EP-0.65	31.5	18.8	12.6	4.3

* τ_{app}-applied shear stress, τ_{max}-shear strength

It is known that adhesives, being viscoelastic materials, deform over the time when they are subjected to sustained loads. This phenomenon is called creep and results in a premature failure even if a small load or stress level is applied. For these adhesives, non-accelerated shear creep tests were performed in [4] and [10] according to the procedure followed by [11] and [12]. The duration of these tests was at least three months, during which epoxy exhibited a creep strength much higher than that of acrylic. According to [13], the displacements measured in the tests have to be extrapolated to 50 years using a given model so that the lifetime of the joints can be predicted. It was found that none of the tested joints can withstand over such a long period of time. Therefore, the lifetime of the bonded joints was only predicted for lifetimes of up to 10 and 25 years and the normalized shear stresses (ratios of the maximum shear stresses) were then proposed for shorter lifetimes as listed in Table 1.

Despite the degradation in the shear strength of the adhesives, bonded joints might be still promising in some specific applications such as for joining thin-gauge lightweight steel members with relatively large bonded areas, as will be illustrated in the next sections.

3 Strengthening cold-formed thin-gauge galvanized steel girders

3.1 Girders studied

The girders studied were cold-formed from 2 mm thick galvanized steel sheets and manufactured as channel sections (C-section) with a length of 1 m. Three girders were fabricated with the geometries shown in Fig. 2. For strengthening the girders, 500 mm long steel plates measuring 35 × 2 mm were cut from 2 mm thick galvanized steel sheet. The first girder was a non-strengthened girder that was tested and used as a reference specimen. The second and third ones were strengthened with externally bonded plates on their upper and bottom flanges attached with a 0.65 mm thick adhesive layer. The girders of this type are called AC-U-B (bonded with acrylic) and EP-U-B (bonded with epoxy). The bonding process was performed according to the manufacturer's recommendations. Twenty-four hours after bonding, 50 mm × 75 mm × 5 mm angles with a length of 30 mm were bonded at the middle of the upper flanges of each girder. Using these angles has two advantages: firstly, they distribute the concentrated force over a width of 30 mm of the top flanges via the horizontal legs of the angles and, secondly, they keep the path of the applied force closer to the

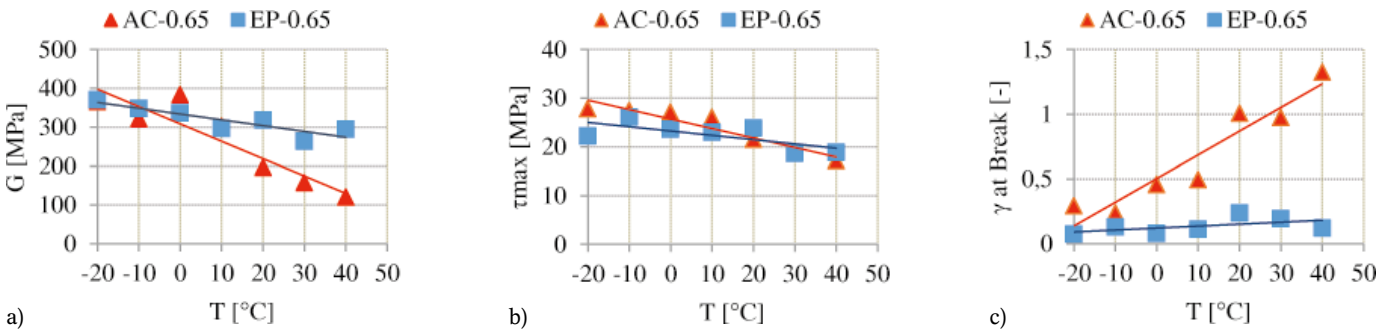

Fig. 1. Shear properties of adhesives plotted against temperature [4]: a) shear modulus, b) shear strength, c) shear strain at break
Bild 1. Schubeigenschaften von Klebstoffen als Funktion der Temperatur [4]: a) Schubmodul, b) Schubfestigkeit, c) Schubdehnung

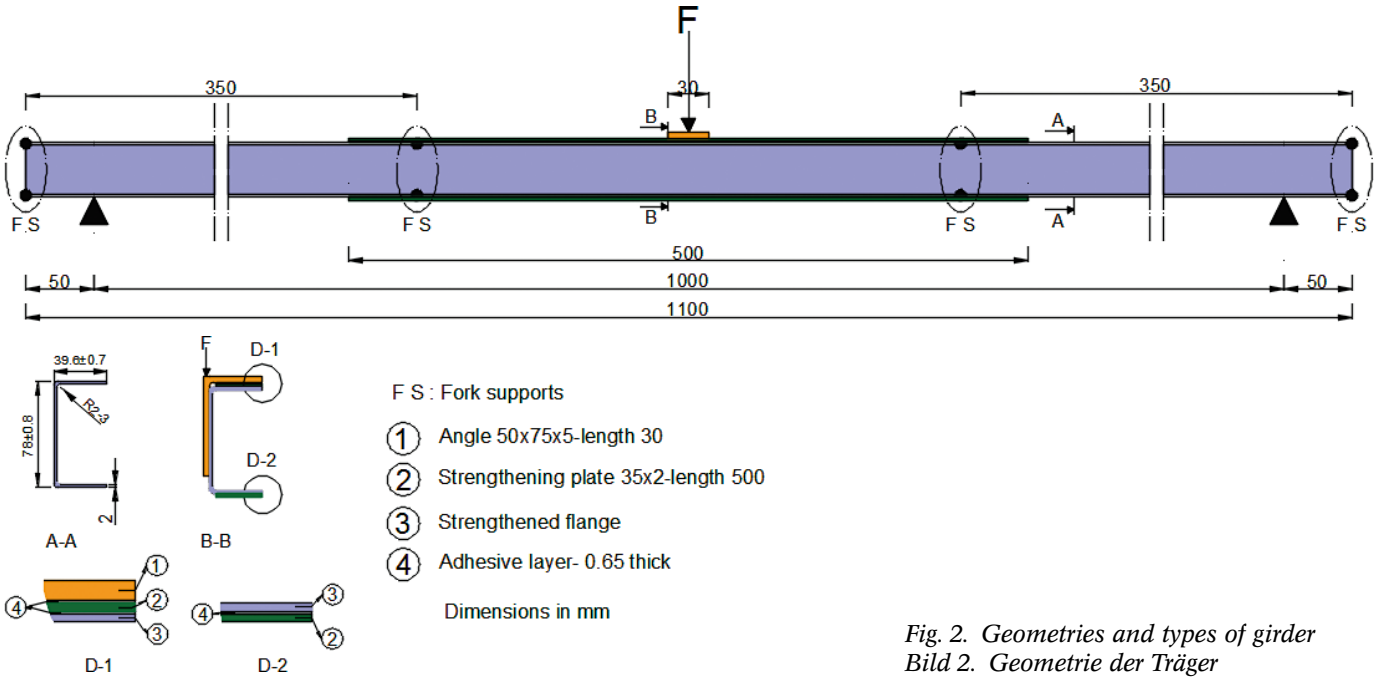

Fig. 2. Geometries and types of girder
Bild 2. Geometrie der Träger

shear centre of the C-section in order to reduce the lateral torsional buckling associated with such unsymmetrical sections (see Fig. 2). The girders were left for five days (AC) and seven days (EP) at room temperature (the curing time needed for each adhesive to be fully cured) and then tested.

3.2 Test setup

A 3-point bending test was used for testing the girders at room temperature. The girders were simply supported during the test. To prevent lateral torsional buckling of the unsymmetrical sections, fork supports were used at four positions over the length of the test girders. The load was applied to the top of the vertical legs of the angles. The feed rate of the crosshead of the compressor was 7.5 mm/min. Deflection at mid-span was measured using linear displacement sensors.

3.3 Test results and observations

As expected, the reference specimen (non-strengthened girder) failed because local buckling occurred close to mid-span (exactly adjacent to the bonded angle), where the moment is a maximum (see Fig. 3). Slight curvature of the girder was noticed. The maximum force carried by the girder was 10.5 kN.

The girders of the second type, i. e. AC-U-B and EP-U-B, started curving noticeably and then lateral torsional buckling occurred between the middle fork supports. The regions adjacent to the strengthening plates started rotating with local buckling-like (see Fig. 4a). No local buckling occurred at mid-span. The bonded plates of EP-U-B separated from the flanges (Fig. 4b), whereas AC-U-B exhibited no separation of the strengthening plates (Fig. 4c). The maximum forces recorded for the girders were 16.1 and 15.7 kN for AC-U-B and EP-U-B respectively.

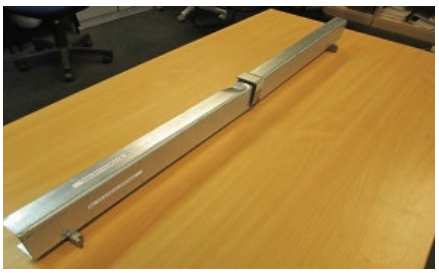

Fig. 3. Deformation of non-strengthened girder
Bild 3. Deformation des nichtverstärkten Trägers

3.4 Numerical investigations

Better understanding of the behaviours of the bonded strengthening joints can be obtained by knowing the stress distributions developing within the adhesive layers. This can be done through numerical investigations employing finite element method-based models. Two models representing the strengthened girders tested at room temperature (AC-U-B, EP-U-B) were built using ABAQUS software. The models have geometries and boundary conditions similar to those shown in Figure 2. The adhesive material was considered as a linear elastic isotropic material. The elasticity modulus E, *Poisson*'s ratio ν and yield strength σ_y of the adhesives are listed in Table 2.

Defining the materials of the steel members in the models was done by using the true stress-strain curves given in [4]. The steel structures (C-section plus strengthening plates) were modelled using 4-node linear quadrilateral shell elements of type S4R; the C-section was meshed into 7 700 elements, the strengthening plate into 700. The layer of adhesive was modelled with 8-node linear hexahedral solid elements of type C3D8R and was meshed into 800 elements. The angles were represented by defining the areas under them as rigid bodies, whereas the force was applied to a defined reference point attached to the rigid body of the angle

Table 2. Material properties of adhesives used in ABAQUS
Tabelle 2. In ABAQUS angenommene Materialeigenschaften der Klebstoffe

	ν	E in MPa	σ_y in MPa
AC-0.65	0.44	565	36.9
EP-0.65	0.38	875	41.4

a) Deformed AC-U-B and EP-U-B girders (left); curvature of the girders (right)
a) verformte Träger AC-U-B und EP-U-B (links); Trägerkrümmung (rechts)

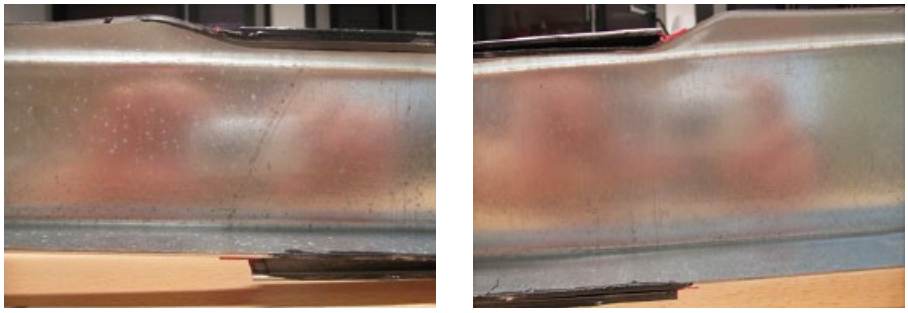

b) Separation of the bonded plates in EP-U-B
b) Trennung der geklebten Platten in EP-U-B

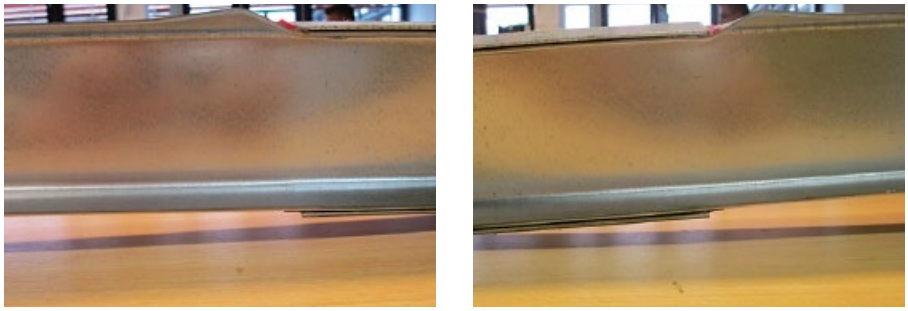

c) No separation of bonded plates in AC-U-B
c) keine Trennung der Platten in AC-U-B

Fig. 4. Deformations of AC-U-B and EP-U-B
Bild 4. Deformationen von AC-U-B und EP-U-B

using the coupling definition. Based on the fact that the joint fails cohesively, i. e. failure takes place in the adhesive layer and not at the interfacial surfaces, the layers of the adhesive were connected with the steel adherends (flange and strengthening plate) using an appropriate definition of contacts based on the theory of the so-called slave and master surfaces [14]. According to EN 1993-1-5 [15], geometrical imperfections were introduced into the numerical models based on the linear solution of the buckling analysis, which resulted in several local buckling modes. Linear combinations of the chosen (local) buckling modes were created after scaling them by adequate factors and then used to provide the models with the new geometries; therefore, new configurations of the models were achieved. These procedures as well as the combinations of each model introduced can be found in [4]. After introducing these combinations, the nonlinear post-buckling analysis using the Riks method was carried out on the newly created models.

3.5 Validation of models

Calibration of the models was carefully done on the basis of the results of the experimental investigations performed. The external load F and the mid-span deflection u were measured. Validation of the models was done by comparing the numerical and experimental results quantitatively and qualitatively. Figure 5 presents the quantitative comparison of the numerical and experimental (F-u) dia-

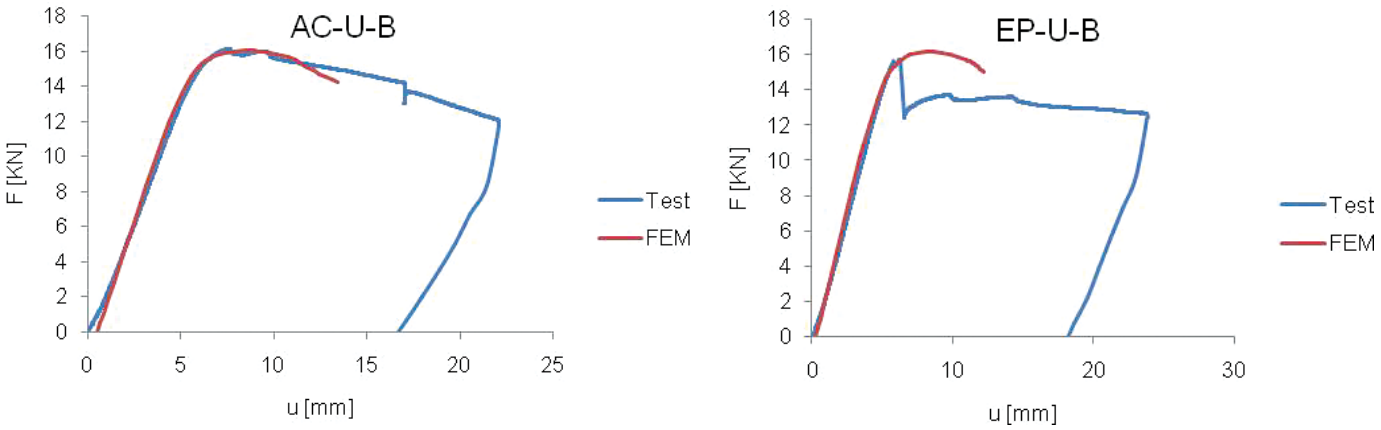

Comparison of AC-U-B: F_{max} (test) = 16.1 kN, F_{max} (FEM) = 16 kN

Comparison of EP-U-B: F_{max} (test) = 15.7 kN, F_{max} (FEM) = 16.2 kN

Fig. 5. Quantitative comparisons between test and FEM results
Bild 5. Quantitativer Vergleich zwischen Testergebnissen und FE-Ergebnissen

grams for the girders investigated. The high conformity of the stiffness of both models and relatively good agreement between the ultimate capacities can be seen. It should be noted that the mismatch in the curves for EP-U-B post-peak can be attributed to the separation of the strengthening plate. Representing such failure needs a special definition of the failure criteria in ABAQUS [14] which is not considered in these numerical investigations. The qualitative validation of the numerical results is shown in Figure 6, which indicates that the deformations of the girders in the numerical simulation are identical to those of the real test shown in Figure 4.

3.6 Investigating temperature effects

The investigations of the temperature effects were performed numerically using the FEM models created for the room temperature tests and validated for use in a parametric study. The temperature effect was therefore introduced into the models by making use of the mechanical properties obtained from small-scale specimens at the temperatures studied [4], i. e. at –20 °C and +40 °C. The properties used are given in Table 3.

3.7 Results of numerical investigations

It was noticed that the F-u diagrams for the girders investigated at the temperatures studied (–20 °C and +40 °C) are identical to those obtained at room temperature (shown in Fig. 5); therefore, they will not be presented again. Consequently, the capacities of the girders have not varied from those reached at room temperature. Moreover, the stresses developing over the adhesive layers are distributed in the same form but with different values according to the temperature.

The *von Mises* stress distributions at room temperature (RT), corresponding to the maximum force F_{max} recorded in FEM calculations, are presented in Figure 7 for the girders strengthened by AC-bonded plates and in Figure 8 for those strengthened by EP-bonded plates.

It is clear that the furthest corners of the adhesive layers are the most highly stressed and that the high stresses are concentrated in the re-

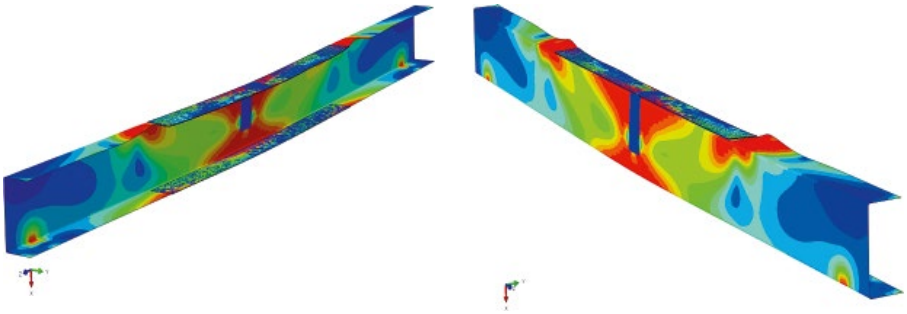

Fig. 6. Qualitative validation of models, deformed shape of girders: front view (left), rear view (right)
Bild 6. Qualitative Validierung der Modelle, deformierter Träger: Vorderansicht (links), Rückansicht (rechts)

Table 3. Material properties of adhesives used in ABAQUS for –20 °C and +40 °C
Tabelle 3. In ABAQUS angenommene Materialeigenschaften der Klebstoffe bei –20 °C und +40 °C

	Temperature in °C	ν	E in MPa	σ_y in MPa
AC-0.65	–20	0.44	1053	51.1
	+40		303	28.9
EP-0.65	–20	0.38	1023	38.5
	+40		812	32.7

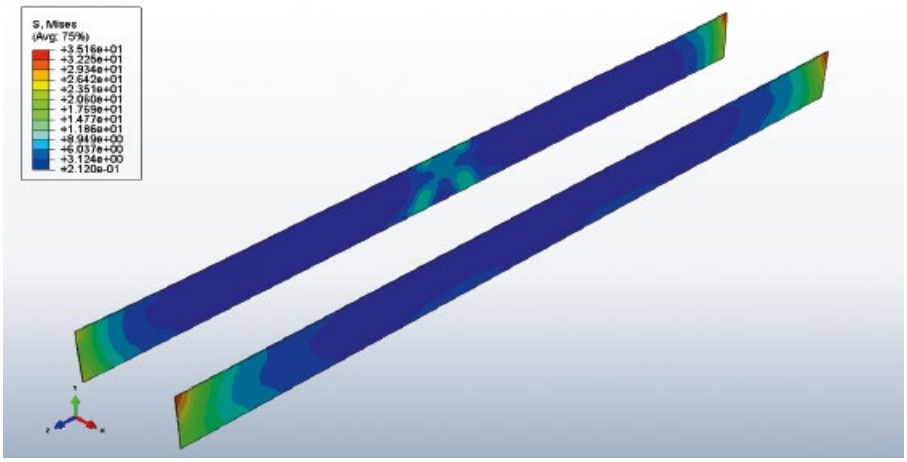

Fig. 7. Von Mises stress in MPa over the adhesive layers in AC-bonded girders
Bild 7. Von Mises-Spannung in MPa in der Klebschicht bei AC

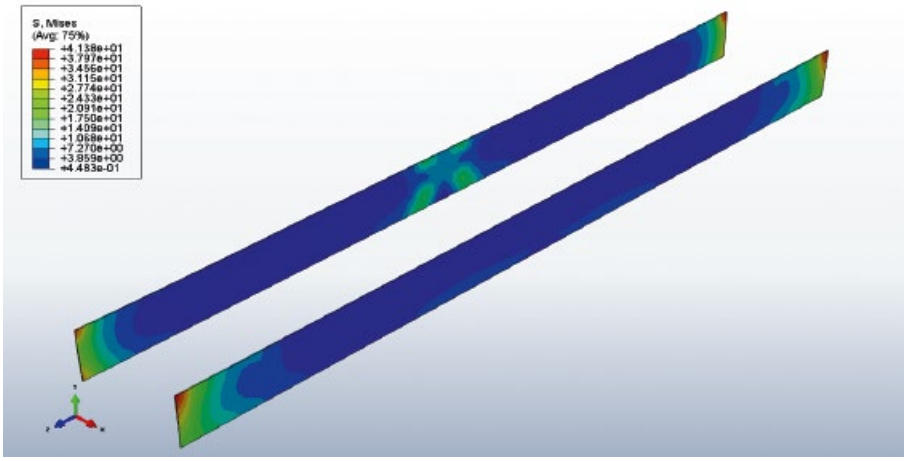

Fig. 8. Von Mises stress in MPa over the adhesive layers in EP-bonded girders
Bild 8. Von Mises-Spannung in MPa in der Klebschicht bei EP

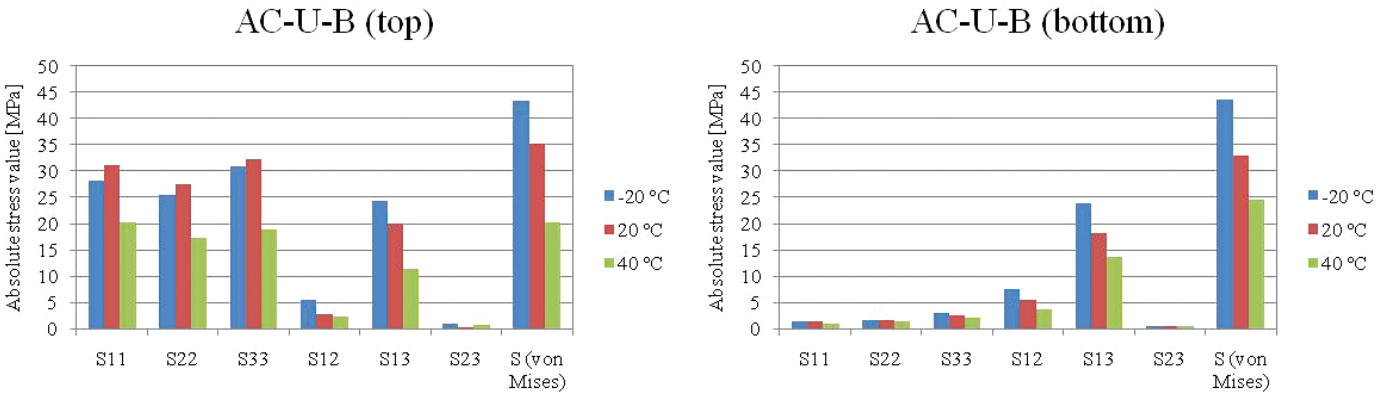

Fig. 9. Absolute stress values in MPa for AC-bonded girders, which correspond to Fmax at the most highly stressed corner of the adhesive layers at the temperatures studied; values at –20 °C, +20 °C and +40 °C are: 51.1, 36.9 and 28.9 MPa respectively
Bild 9. Absolute Spannungswerte in MPa für AC-geklebte Träger

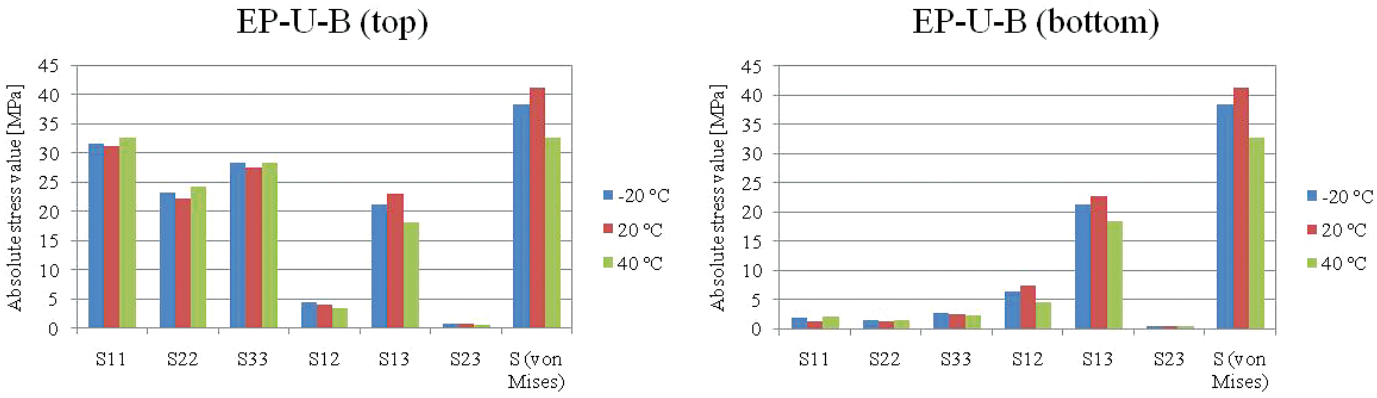

Fig. 10. Absolute stress values in MPa for EP-bonded girders, which correspond to Fmax at the most highly stressed corner of the adhesive layers at the temperatures studied; values at –20 °C, +20 °C and +40 °C are: 38.5, 41.4 and 32.7 MPa respectively
Bild 10. Absolute Spannungswerte in MPa für EP-geklebte Träger

gions 5 mm to 10 mm wide which are very close to the edges, whereas the stresses acting between these regions are relatively small.

It is well understood that in lap bonded joints, the normal stresses S11 and shear stresses developing parallel to the adhesive layer S13 are concentrated at the ends of the adhesive layers. However, the concentration of all normal stresses (S11, S22, and S33) have increased in the layers used at the top due to the rotations occurring in the top flanges beside the strengthening plates (see Fig. 9a for AC-bonded girders and Fig. 10a for EP-bonded girders). This is obvious when these stresses are compared with the corresponding stresses developing over the bottom adhesive layers (see Fig. 9b and Fig. 10b for AC-bonded and EP-bonded girders respectively).

4 Discussion and conclusion

It was found that the maximum *von Mises* values for the AC-bonded girders at the three temperatures studied are still lower than the yield strengths of the AC adhesive. This explains why no separation of the bonded plates occurred during the test at room temperature and also indicates the efficiency of these materials when used over the temperature range considered. On the other hand, the separation in the girders bonded with EP (EP-U-B) is probable at the three temperatures since the yield strength of epoxy has been reached. This also explains the separations of the bonded plates which occurred during the test at room temperature.

Comparing EP-U-B with AC-U-B girders reveals that the bonded plates separated in EP girders a little before reaching the maximum capacity achieved when using AC adhesive (15.7 kN for EP and 16.1 kN for AC), making only a 4 % difference in the increase in capacity. This can be attributed to the fact that the separation of the bonded plates was approximately at the same time as the failure of the C-sections outside the strengthened regions.

The reason that the yield strength of EP was reached before that of AC at +20 °C and +40 °C, although it is higher than the AC value, is that at these temperatures the rigidity of EP is greater but its ductility is less (see Tables 2 and 3 and Figs. 1a and 1c), so the deformation of EP is limited compared with that of AC, which can deform easily, absorbing the deformations of the ductile steel. At –20 °C it can be attributed to the fact that AC is almost as rigid as EP

with a higher yield strength and greater ductility.

Based on the experimental and numerical results, the following conclusions can be drawn:

- Strengthening the C-section girders by bonding additional plates to their flanges was able to increase the capacity of the girders by about 50 to 54 %. The local buckling problem at the mid-span of the compressed thin-gauge flanges was overcome by the bonded strengthening joints.
- It was found that the temperature-dependent properties of the adhesive materials do not play any effective role in changing the behaviour of the strengthened girders nor their capacities because the separation of the strengthening plates takes place almost at the same time as the occurrence of the dominating failures of the C-section girders.
- In order to absorb the deformations of the ductile steel sheets, the preferred adhesive for use in their joints is the ductile one (acrylic adhesive, AC) since it is easier to deform it without breaking it.
- Since the *von Mises* stress acting over most of the adhesive layers (blue areas in Figs. 7 and 8) is very small, the dominant stresses (i. e. the shear stresses) will be even smaller and much less than those proposed for the lifetimes presented in Table 1, which implies that the creep phenomenon will have a negligible influence.

Acknowledgements

This work was carried out with financial support provided by the German Academic Exchange Service (DAAD).

References

[1] *Pasternak, H., Meinz, J.*: Versuche zu geklebten Verstärkungen im Stahlhochbau. Bauingenieur 81 (2006), S. 212–217.

[2] *Pasternak, H., Piekarczyk, M., Kubieniec, G.*: Adhesives in strengthening of steel structures. Statybinės Konstrukcijos ir Technologijos, vol. 2 (2010), No. 2, pp. 45–50.

[3] *Pasternak, H., Meinz, J.*: Kleben im Stahlbau – zwei Beispiele aus dem Fassadenbau. Bauingenieur 82 (2007), S. 115–124.

[4] *Sahellie, S.*: Study on the temperature effect on lap shear adhesive joints in lightweight steel construction. Doctoral thesis. Brandenburg University of Technology, Cottbus, Germany. Schriftenreihe Stahlbau 2015, Heft 9.

[5] *Pasternak, H., Sahellie, S.*: Conversion factors of the temperature effect on the shear strength of adhesively-bonded steel joints. Journal of Civil Engineering and Management, in press (2015).

[6] EN 1990:2002: Eurocode – Basis of structural design.

[7] ISO 2394:1998: General principles on reliability for structures.

[8] *Van Straalen, I. J., Van Tooren, M. L.*: Development of design rules for adhesive bonded joints. HERON 47 (2002), No. 4.

[9] *Van Straalen, I. J.*: Development of design rules for structural adhesive bonded joints – A systematic approach. PhD thesis, Delft University of Technology, The Netherlands, 2001.

[10] *Sahellie, S., Pasternak, H.*: Expectancy of the lifetime of bonded steel joints due to long-term shear loading. Archives of Civil and Mechanical Engineering, in press (2015).

[11] *Meshgin, P., Choi, K., Taha, M.*: Shear creep of epoxy at the concrete-FRP interfaces. ScienceDirect, vol. Part B 38 (2007), pp. 772–780.

[12] *Meshgin, P., Choi, K., Taha, M.*: Experimental and analytical investigations of creep of epoxy adhesive at the concrete-FRP interfaces. International Journal of Adhesion & Adhesives 29 (2009), pp. 56–66.

[13] ETAG 001: Guideline for European Technical Approval of metal anchors for use in concrete – Part 5: Bonded Anchors, 2008.

[14] ABAQUS, user's manual, version 6.11-3, 2011.

[15] EN 1993-1-5(2006): Eurocode 3 – Design of steel structures – Part 1-5: Plated structural elements.

Autoren dieses Beitrages:
Dr.-Ing. Samer Sahellie, MSc,
samer.sahellie@b-tu.de,
Prof. Dr.-Ing. habil. Hartmut Pasternak,
hartmut.pasternak@b-tu.de,
Brandenburg University of Technology,
K.-Wachsmann-Allee 2,
03046 Cottbus